

ANL/ET/CP--79615
Conf 9310111--2

TMI-2 Instrument Nozzle Examinations at Argonne National Laboratory*

by

L. A. Neimark
T. L. Shearer
A. Purohit
A. G. Hins

CONFIDENTIAL

OCT 19 1993

OSTI

Energy Technology Division
Argonne National Laboratory
Argonne, IL 60439

The submitted manuscript has been authored by a contractor of the U.S. Government under contract No. W-31-109-ENG-38. Accordingly, the U.S. Government retains a nonexclusive, royalty-free license to publish or reproduce the published form of this contribution, or allow others to do so, for U.S. Government Purposes.

September 1993

This report was prepared as an account of work sponsored by an agency of the United States Government. Neither the United States Government nor any agency thereof, nor any of their employees, makes any warranty, express or implied, or assumes any legal liability or responsibility for the accuracy, completeness, or usefulness of any information, apparatus, product, or process disclosed, or represents that its use would not infringe privately owned rights. Reference herein to any specific commercial product, process, or service by trade name, trademark, manufacturer, or otherwise does not necessarily constitute or imply its endorsement, recommendation, or favoring by the United States Government or any agency thereof. The views and opinions of authors expressed herein do not necessarily state or reflect those of the United States Government or any agency thereof.

DISCLAIMER

*Work Sponsored by the U.S. Nuclear Regulatory Commission under an Agreement with the U.S. Department of Energy, Contract W-31-109-Eng-38.

To be submitted for publication in the Proceedings of the Symposium on Achievements of the OECD Three Mile Island Vessel Investigation Project, Boston, MA, October 20-22, 1993.

MASTER

TMI-2 Instrument Nozzle Examinations at Argonne National Laboratory*

L. A. Neimark

T. L. Shearer

A. Purohit

A. G. Hins

Argonne National Laboratory - Illinois

Abstract

Six of the 14 instrument-penetration-tube nozzles removed from the lower head of TMI-2 were examined to identify damage mechanisms, provide insight to the fuel relocation scenario, and provide input data to the margin-to-failure analysis. Visual inspection, gamma scanning, metallography, microhardness measurements, and scanning electron microscopy were used to obtain the desired information. The results showed varying degrees of damage to the lower head nozzles, from $\approx 50\%$ melt-off to no damage at all to near-neighbor nozzles. The elevations of nozzle damage suggested that the lower elevations (near the lower head) were protected from molten fuel, apparently by an insulating layer of fuel debris. The pattern of nozzle damage was consistent with fuel movement toward the hot-spot location identified in the vessel wall. Evidence was found for the existence of a significant quantity of control assembly debris on the lower head before the massive relocation of fuel occurred.

*Work Sponsored by the U.S. Nuclear Regulatory Commission under an Agreement with the U.S. Department of Energy, Contract W-31-109-Eng-38.

INTRODUCTION

Fourteen instrument tube nozzle segments were removed from the lower head of the TMI-2 reactor for detailed examinations as part of the Vessel Integrity Project (VIP). Six of these were examined at Argonne National Laboratory-Illinois (ANL) and eight were to be examined at the EG&G Idaho National Engineering Laboratory (INEL). The purpose of the nozzle examinations at ANL was to (1) provide information on the temporal and locational movement of fuel onto and across the lower head; (2) estimate peak temperatures of the nozzles from their metallurgical end-state; and (3) determine the mechanisms, modes, and extent of nozzle degradation to evaluate the imperilment of the lower-head containment boundary. Corollary objectives to focus the examinations were (1) determine the nature and extent (axial and radial) of fuel/debris ingress into a nozzle; (2) determine the nature and degree of chemical and thermal interaction between fuel, debris, and nozzles; (3) determine thermal-related metallurgical changes in the nozzle as a function of axial position to evaluate the axial temperature distribution and attempt to quantify temperatures near the vessel; and (4) determine the position and composition of debris adhering to nozzle surfaces to establish a "debris bed depth".

The nozzle segments received at ANL were from locations D10, E11, H5, H8, L6, and M9. Figure 1 shows the location of these nozzles in the reactor grid plan. These nozzle segments represented a range of thermal damage, i.e., melt-off and surface degradation, found in the fourteen nozzles during the removal operations. Nozzles in the area of E-F/7-9 were significantly more damaged than the peripheral nozzles. The degree of damage to individual nozzles would be indicative of the possible damage, or change in metallurgical condition, of the vessel in proximity to the nozzle. The H8 nozzle was the most heavily damaged of those examined at ANL, having a length of only 70 mm atop a residual stub left on the vessel of only 51 mm. The L6 nozzle, on the other hand, was 241 mm long and showed no outward appearance of any damage. The other four nozzles had either melt-off damage at different elevations (M9 and H5) or different degrees of surface damage (D10 and E11). Thus, the examination of these six nozzles would provide information and insight to satisfy all of the objectives of the examinations.

The detailed results of these nozzle examinations are reported in Ref. 1. Only the most significant findings will be summarized in this paper.

EXAMINATION METHODS

The examination tools used at ANL consisted of visual examination and macrophotography, axial gamma scanning for ^{137}Cs , macroexamination of cut sur-

faces, metallography, microhardness measurements, and scanning electron microscopy/energy dispersive X-ray (SEM-EDX) analysis.

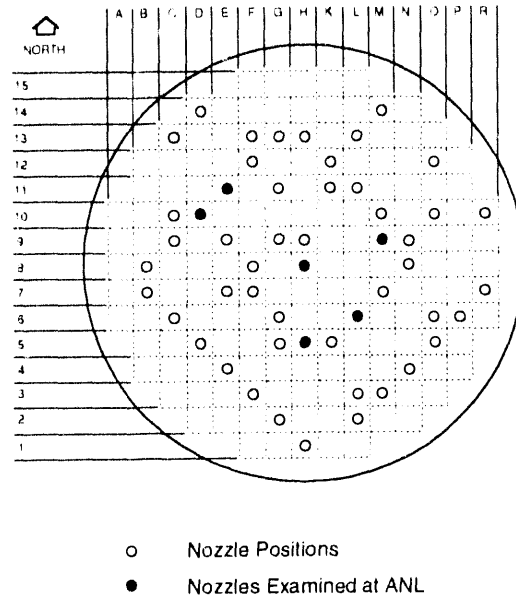


Fig. 1. Grid Map of TMI Core Showing Locations of Nozzles Examined at ANL

The nozzle segments were systematically sampled for detailed examination to obtain the desired data. The areas sectioned were based on the following attributes: (1) top and bottom locations to obtain information on the hottest (sometimes molten) and coldest (nearest the vessel) temperature extremes in a nozzle; (2) fuel/nozzle interaction areas (nozzle degradation mechanism); (3) indications from gamma scans of fuel penetration into the nozzle; (4) obvious locations of surface layers on a nozzle; and (5) locations of surface cracking (nozzle degradation mechanism).

SIGNIFICANT FINDINGS

Pattern of Nozzle Damage - To appreciate the significance of the damage findings, the elevation of the damage to a particular nozzle above the bottom of the vessel must be considered. Figure 2 shows the relationships between the elevations of nozzle locations referenced to the lowest nozzle location at H8, while Table 1 provides the actual elevations and segment lengths for the six ANL nozzles. These elevations are important to the understanding of the man-

ner in which molten fuel debris moved on the lower head and caused the nozzle damage. Figure 3 shows the as-removed appearance of the six ANL nozzles. The tops of nozzles M9 and H5 were clearly melted off an appreciable amount. The transition zone between the molten region and the unaffected lower part of the nozzles was relatively narrow on M9 and more extensive on the shorter H5. These transition zones were typically covered with a thin scale that was basically an iron oxide with entrapped shards of various core debris materials (Fig. 4); the lower areas of the nozzles were clean of adherent scale and showed little, if any, effects of being in contact with very hot core debris.

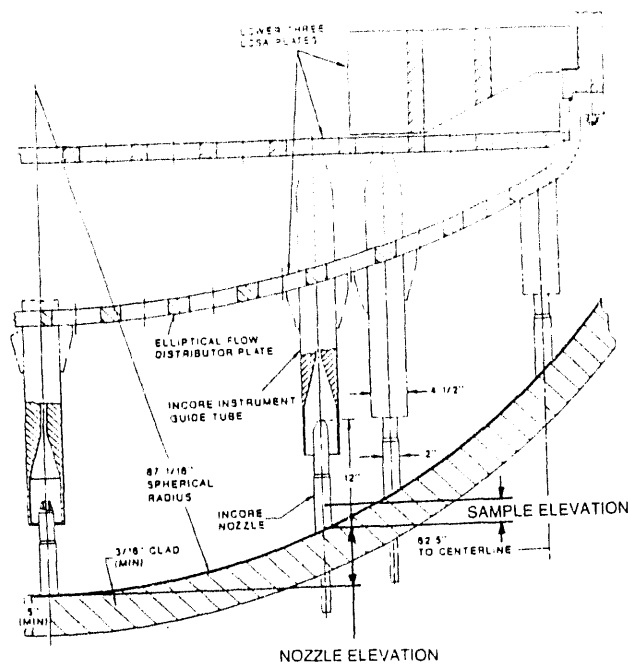


**Fig. 2. Lower-head Area and In-core Instrument Guide Tubes.
(MPR No. F-73-30-311)**

Significant fuel penetration into these molten nozzles was essentially limited to the melted and scaled elevations, i.e., the hot top of the nozzle. The material found in the top of nozzle M9, Fig. 5, was a mixture of solidified fuel and nozzle remnants in a matrix of chromium-oxide, from the Inconel 600 nozzle material, different from the Fe-based oxide scale on the outside of the nozzles. It is believed that the downward mobility of the trapped fuel was dominated, and limited, by the Cr-oxide (Cr_2O_3 melts at 1990°C).

Table 1. ANL Nozzle Segment Lengths, Elevations, and Fuel Penetration Depths

Nozzle	Elevation of Nozzle Base, mm	Segment Length, mm	Stub Length, mm	Elevation of Top of Segment, ^a mm	Fuel Penetration Elevation above Nozzle Base, ^b
M9	119	254	26 ^c	280	241
L6	94	241	64 ^c	305	75
H5	107	146	0	146	89 max 117 min
H8	0	70	51	121	<64
D10	244	235	57 ^c	292	55 max 184 min
E11	221	225	77 ^c	302	204

^aReferenced to nozzle base.

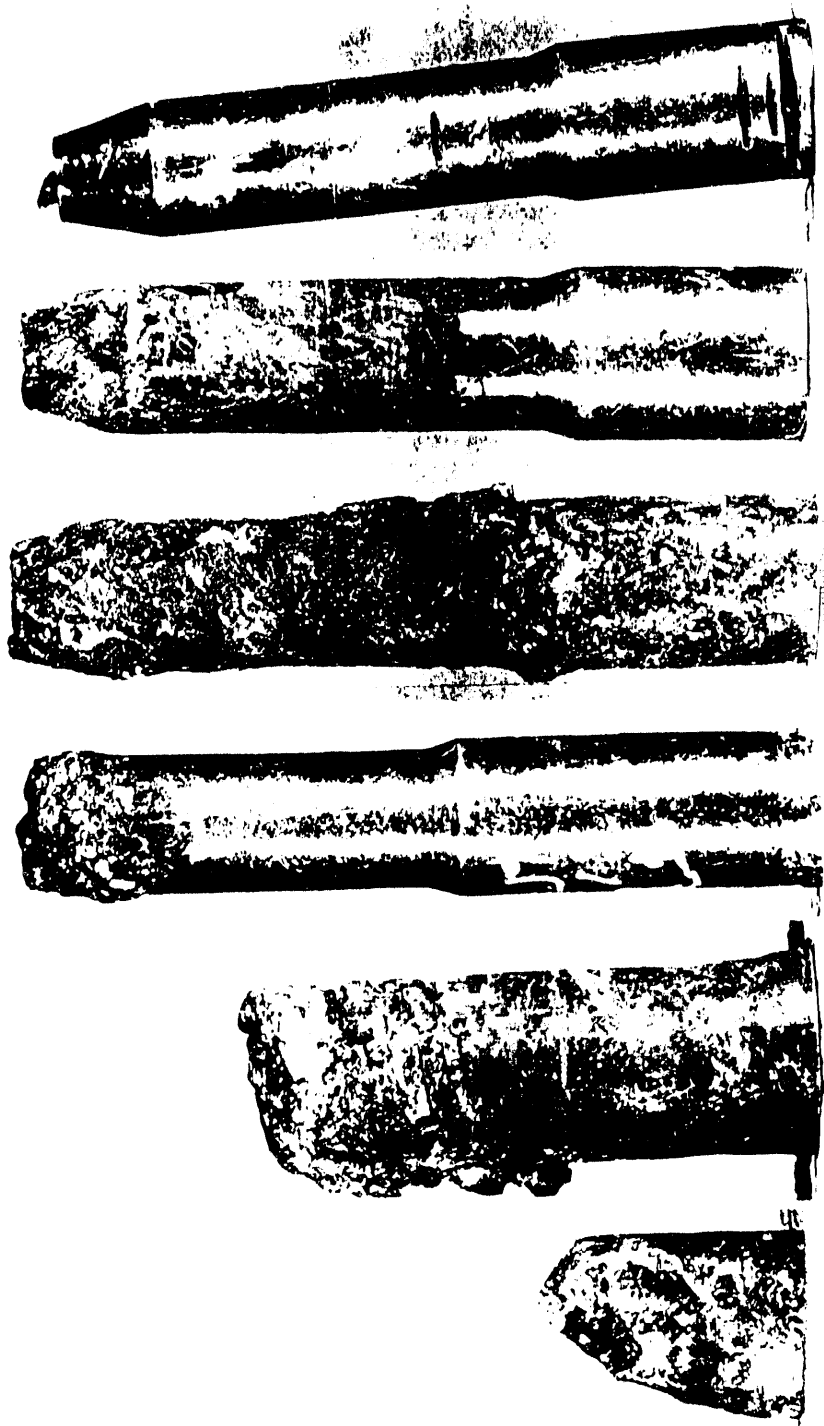
^bBased only on gamma scans.

^cCalculated as the difference between 305 mm and the sum of the two known values.

Measurements of stub lengths for D10 and E11 from photographs were not deemed sufficiently accurate because of angle of photo.

The H8 nozzle segment received at ANL was only the bottom portion of a longer post-accident segment, the top of which was broken off during the removal operations. The top surface of the bottom portion, shown in Fig. 3, was smooth compared to the melted regions of M9 and H5. Upon detailed examination by SEM-EDX, it was found that this surface had been reacted extensively with a molten Zr-rich phase which contained ingots of Ag-Cd. These elements would have come from control assembly components that apparently melted early in the accident and deposited on the lower head in advance of the major fuel flow there. Intergranular penetration of Ag-Cd was found in a number of nozzles and into the surface of the vessel.²

In contrast to the melted condition of nozzles M9 and H5, nozzle L6, almost midway between them on the lower head, showed no external damage at all. This indicates that the fuel movement in the lower head was not one unified flow, but rather individual flows coming from different directions.



L6

E11

D10

M9

H5

H8

Figure 3. Appearance of Nozzles As-removed from the Lower Head.



Fig. 4. Layer of Debris on Outer Surface of D10 at the 82-mm Elevation.
(190X, 281852)

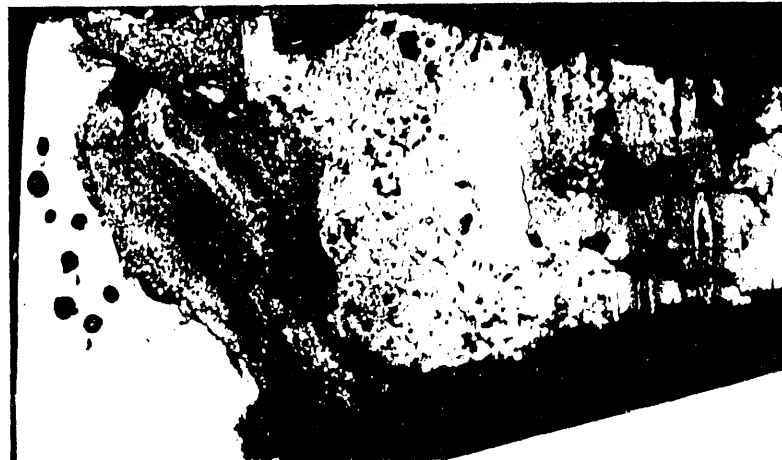


Fig. 5. Longitudinal Section Through Top of Nozzle M9 (7X).

Although the surface of nozzle L6 was clean, the nozzle contained solidified fuel masses down to within 75 mm of its base, the deepest penetration in any nozzle. This deep penetration is attributed to the lack of fuel/nozzle interaction that would have formed a binding Cr-oxide. Because both the nozzle and its overlapping guide tube were undamaged, the source of this fuel is not obvious in that it appears to have been physically impossible for molten fuel to have come up under the guide tube and down into the nozzle without damaging either. It must be concluded that the fuel came down directly through the guide tube from somewhere up in the reactor.

Nozzle D10 was a peripheral nozzle that appears to have been on the edge of the flow of molten fuel. One side of the nozzle was heavily crusted over its entire height, while the other side, in a 180° arc, showed only the more common light surface scale. Upon sectioning it was found that an unexplained internal pressurization had pushed out the hot, crusted side of the nozzle making it egg-shaped in cross section. The internal pressure created a crack in the outer surface of the nozzle and had also collapsed the inner Inconel 600 tube of the instrument string. The body of the nozzle had undergone intergranular hot-tearing, which apparently penetrated to the surface and formed the crack. The non-uniform damage indicates that it occurred quickly, with no time for heat transfer to the rest of the nozzle. This could be expected at the edge of a fuel flow coming to rest up against the nozzle.

The last nozzle, E11, was damaged only at its tip, below which was a fairly extensive area of the Fe-based scale. Melting was limited to the inner and outer surfaces of the tip, with indications of rapid melting and solidification. Fuel penetration was relatively deep, compared to that in M9, apparently because the temperature at the top was too low to form Cr-oxide, which likely would have bound up downward fuel movement. Instead, the material in the tip of the nozzle was in an Fe-based oxide, similar to that of the surface scales.

Two principal points may be concluded from the variable degradation of the instrument tube nozzles. First, considering that most of the nozzles on the lower head were covered with a hard, solidified layer of fuel debris, but that nozzles such as L6 sustained no outward damage from contacting this debris, it can be concluded much of this debris acted as an insulator, and protector, of both the nozzles and the lower head. The absence of virtually any indication of degradation in the bottom parts of even nozzles whose tops had melted indicates that what was likely the first fuel debris to reach the lower head solidified relatively quickly and built up a significantly thick insulating layer. Once this layer had built up it was the later material to arrive on top of the initial material that melted off the tops of those nozzles that were exposed. The elevations at which these melt-offs occurred provides evidence for the thickness of the initial protective layer at various locations around the lower head. Thus, because the

nozzles in the vessel hot-spot area of E-F/7-9 were melted down the most indicates only an initially thin insulating layer existed there, which apparently was the reason the hot-spot formed where it did.

The second point that may be concluded is that the fuel debris movement across the lower head was not one massive, unidirectional flow, but rather more likely, a number of flows from different directions. This derives from the lower head locations where specific nozzles melted off and the elevations at which they melted. The melt-off of M9, in the eastern side of the lower head, at a relatively high elevation indicates a thick initial layer there with the subsequent hot fuel moving downward toward the reactor center off this thick crust. Similarly, nozzles H5 and G5 were melted off atop a somewhat thinner initial crust, whereas nozzle L6 did not melt because it was totally covered initially with relatively cold debris. These crust thicknesses are likely indicative of the amount of material that initially fell on these locations, and indeed these locations correlate with the locations in the elliptical flow distributor through which debris is believed to have come. Debris flowing downward atop initial crusts at M9 and H5 would effectively be going toward the grouping of short, melted-off nozzles where the vessel hot-spot occurred.

Penetration of Materials into Nozzles - The penetration of gamma-active materials downward into the nozzles was estimated from the ^{137}Cs gamma activity profiles and the results are summarized in Table 1. It was assumed that the gamma activity was associated with fission products in fuel and, therefore, the results are reported as "fuel penetration." Metallic debris, essentially molten Inconel from the nozzle, were also found in the nozzles, but not tabulated.

Although porous, ceramic-appearing material was seen in the as-cut transverse sections at elevations below the nozzle tops, such as in H8 and L6, there seemed to be difficulty in retaining it during the subsequent sectioning operations to form metallographic mounts. This would attest to the friable nature of the material. Fuel material that was retained at the lower elevations in most cases had two features. First, it appeared to be in the early stages of transformation to U-rich and Zr-rich phases, indicating relatively rapid cooling. Second, it contained Fe, Al, and Cr in the grain boundaries, indicating likely fluidity significantly below 2000°C. That would aid the fuel's mobility to the elevation where it finally solidified.⁴

In nozzles M9 and H5, which melted off, the penetration was shallow, indicating a quick melting and relatively rapid cooling, the phase transformations in the fuel areas notwithstanding. It is likely that the melting point of Cr-oxide dominated the mobility of this material before thermal equilibrium and lower-melting eutectics could form. The phase transformation of the fuel would have

occurred below 1990°C while the solidified fuel was trapped in the insulating Cr-oxide.

The fuel in the tops of D10 and E11 differed from that in M9 and H5 in that it was trapped in an Fe- rather than a Cr-based matrix. This reflects two things. First, the Inconel did not readily give up its Cr to oxidation, probably because the temperature was too low. Second, the source of the fuel and the Fe-based matrix was probably the same as that of the Fe-based surface scales. That many of the fuel particles were shards and not solidified in-situ masses indicates that the fuel flow in this region of the vessel was cooler than the flow that contacted M9, H5, and H8. This is consistent with a scenario that has the fuel flow coming to the vessel hot spot from the east and south and piling up on the far side against D10 and E11. (Note that the surface crust and major heating load was only on one side of D10.)

Presence of Control Assembly Materials - Four of the six nozzle segments examined at ANL were under control rod assemblies: M9, L6, H5, and H8. One, D10, was beneath an axial power shaping rod that contained 914 mm of Ag-In-Cd clad in stainless steel. The last, H5, was beneath a burnable poison rod that contained $\text{Al}_2\text{O}_3\text{-B}_4\text{C}$ pellets clad in Zircaloy. There is pervasive evidence from the ANL examinations that materials from assemblies containing Ag-In-Cd deposited in some form, probably as solid particulates, on the lower head before the principal fuel flow occurred at 226 minutes. Unfortunately, there is no direct, unequivocal evidence that a control rod debris bed existed on the lower head. Most, if not all, of such a control rod debris bed would have re-melted when it came in contact with even the initial, cooler fuel that reached the lower head first; possibly it would have been consumed into it. Therefore, evidence for such a bed would now be, at best, on a microscopic scale and fortuitously derived.

The first evidence that the control materials were on the lower head before the fuel flow arrived was the finding of Ag-Cd nodules and In-Fe-Ni-Zr phases solidified in situ in the vessel cladding cracks in the E6 and G8 boat samples.² Second, the liquid that ablated nozzle H8 was overwhelmingly Zr-rich and contained Ag-Cd masses. The Zr:U ratio of $\approx 8.5:1$ was far in excess of the Zr/U ratios found in fuel masses that were analyzed. This excess of Zr would be from the Zircaloy shroud tubes in the control assemblies. The minimum depth of the Zr-containing debris bed at this location would have been ≈ 120 mm.

Third, the findings of Ag and Ag-Cd inclusions deep beneath the surfaces in most of the nozzles in a form of liquid metal penetration indicates that there was a layer of control materials either adhering to the surface ready to be melted when contacted by the hot fuel, or there was a thick debris bed up against the nozzle that would yield the same result. That liquid Ag-Cd had penetrated the Inconel nozzles somewhat before nozzle melting occurred is evi-

denced by the apparently vapor-pressure-derived bubbles containing Ag-Cd deposits in the molten Inconel tops of some nozzles. And last, the finding of a layer of 10- μ particles of Ag-Cd beneath a fuel debris scale on nozzle E11.

The significance of a control material debris bed could be two-fold. First, the intergranular penetration of the vessel cladding by Ag-Cd may have played a role in the hot-tearing of the cladding. And second, its interaction with the nozzle material was a low-elevation degradation mechanism that may have allowed greater penetration of molten fuel into nozzle H8 than otherwise would have occurred. A third consideration, a significant insulating effect of the debris bed on the thermal impact to the vessel, could not be supported by a heat transfer analysis.

CONCLUSIONS

The following relevant conclusions were reached from the nozzle examinations:

1. The nature of the degradation of nozzles M9, H5, and H8 indicate that their melt-off was by liquid fuel coming at the nozzles at an elevation ranging from \approx 140 to 270 mm above the lower head. Surface scale on the nozzles below the melt-offs suggests that the liquid was atop a crust of solidified and partially solidified fuel debris that had been cooled below its solidus by contact with the lower head.
2. The flow of very hot material on the lower head followed multiple paths. nozzles M9, H5, and H8 suggest that flows occurred from the east and south, but apparently did not affect nozzle L6 because it had already been covered by cooler material that reached the lower head first.
3. The fuel debris in and on nozzles D10 and E11 and the one-sided degradation of D10 suggest that these nozzles were at the periphery of the fuel flow, likely on the cooler far side.
4. The pattern of nozzle degradation and the assumed fuel flow directions are consistent with a vessel hot spot at E-F/7-8 where there apparently was little initial protective crust.
5. Significant nozzle temperatures ranged from 1400°C (melting) at 140 mm from the vessel at H5, down to \approx 1000°C, based on Ni-Zr eutectic temperature of 961°C, at 64 mm from the vessel at H8.
6. In addition to melting, nozzle degradation mechanisms were ablation by liquid Zr, intergranular penetration by Zr and Ag-Cd, chemical interaction

with Al, Cr-depletion caused by extensive oxidation, and internal pressurization causing hot-tearing and nozzle ballooning.

7. The presence of significant quantities of Zr and Ag-Cd on the vessel to interact with the nozzles is attributed to the prior deposition at that location of control assembly debris. The depth or nature of such a debris bed could not be confirmed, but the depth is estimated to have been a minimum of 120 mm at the H8 location.
8. Fuel debris penetration downward into the nozzles was influenced by the temperature of the fuel at the time of entry; its composition, and hence fluidity; the temperature of the nozzle and its ability to solidify the debris; and the degree of interaction between the fuel and the molten nozzle in entrapping the fuel in Cr-oxide.

ACKNOWLEDGMENTS

The authors acknowledge the support of A. Rubin, C. Serpan, and E. Hackett of the NRC during the course of this work. The endeavors of J. Sanecki for his consultations on analytical results; D. Pushis, W. Kettman, F. Pausche, D. Evans, and L. Essenmacher for photography, specimen preparation, and metallography; and E. Hartig for manuscript preparation are gratefully acknowledged. The authors sincerely thank D. Diercks and T. Kassner for their consultations.

REFERENCES

1. L. A. Neimark, et al., "TMI-2 Instrument Nozzle Examinations at Argonne National Laboratory," TMIV(93)AL01 (February 1993).
2. D. Diercks and L. A. Neimark, "Mechanical Properties and Examination of Cracking in TMI-2 Pressure Vessel Lower Head Material," in Proceedings of the Achievements of the OECD Three Mile Island Vessel Investigation Project, Boston MA, October 20-22, 1993, and "Results of Mechanical Tests and Supplementary Microstructural Examinations of the TMI-2 Lower Head Samples," TMIV(93)AL02 (June 1993).
3. J. R. Wolf, et al., "Lower Head Relocation Scenario," in Proceedings of the Achievements of the OECD Three Mile Island Vessel Investigation Project, Boston MA, October 20-22, 1993, and "TMI-2 Vessel Investigation Project Integration Report, TMIV(93)EG10 (September 1993).
4. R. V. Strain, L. A. Neimark, and J. E. Sanecki, "Fuel Relocation Mechanisms Based on Microstructures of Debris," Nucl. Technol. 87, No. 1 (187-190), August 1989.